

1 **Analytical and numerical assessment of the effect of highly conductive inclusions**
2 **distribution on the thermal conductivity of particulate composites**

3 **Kamran A. Khan,^{1*}, Falah A. Hajeri,² Muhammad A. Khan³**

4
5 ¹*Department of Aerospace Engineering, Khalifa University of Science and Technology,*
6 *Abu Dhabi, UAE*

7 ¹*Department of Mechanical Engineering, Khalifa University of Science and Technology,*
8 *Abu Dhabi, UAE*

9 ²*School of Aerospace, Transport and Manufacturing, Cranfield University, UK*

10
11 *Corresponding author: kamran.khan@ku.ac.ae

12
13 **Abstract**

14 Highly conductive composites have found applications in thermal management, and the
15 effective thermal conductivity (ETC) plays a vital role in understanding the thermo-mechanical
16 behavior of advanced composites. Experimental studies show that when highly conductive
17 inclusions embedded in a polymeric matrix the particle forms conductive chain that drastically
18 increase the ETC of two-phase particulate composites. In this study, we introduce a random
19 network three dimensional (3D) percolation model which closely represent the experimentally
20 observed scenario of the formation of the conductive chain by spherical particles. The prediction
21 of the ETC obtained from percolation models is compared with the conventional micromechanical
22 models of particulate composites having the cubical arrangement, the hexagonal arrangement and
23 the random distribution of the spheres. In addition to that, the capabilities of predicting the ETC
24 of a composite by different analytical models, micromechanical models, and, numerical models
25 are also discussed and compared with the experimental data available in the literature. The results
26 showed that random network percolation models give reasonable estimates of the ETC of the
27 highly conductive particulate composites only in some cases. It is found that the developed
28 percolation models perfectly represent the case of conduction through a composite containing

1 randomly suspended interacting spheres and yield ETC results close to Jeffery's model. It is
2 concluded that a more refined random network percolation model with the directional conductive
3 chain of spheres should be developed to predict the ETC of advanced composites containing highly
4 conductive inclusions.

5 **Keywords:** Effective thermal conductivity, two phase-composites, particulate composites, the
6 distribution of inclusions, highly conductive composites.

7 **1. Introduction**

8 Particulate composites are widely used in thermal storage management, and there is an
9 increasing demand for efficient and highly conductive particulate composites in electronic
10 packaging, heat sinks, and other appliances. The heat transfer capability of particulate composites
11 can be improved by varying spatial distribution of the inclusions and thermal properties of the
12 constituents ([1],[2]). Recently, experimental studies showed that when highly conductive
13 inclusions are embedded in a less thermally conductive matrix, the effective thermal conductivity
14 (ETC) of the composite increases significantly with the increase of volume fraction (V_f) of the
15 inclusions [3]–[7]. A precise model capable of predicting the ETC of the highly conductive
16 particulate composites plays a significant role in evaluating the thermal and stress analysis of
17 advanced composites.

18 The ETC of two-phase isotropic composites depends on characteristics of the constituents such
19 as shape, geometry, spatial distribution, thermal conductivities, V_f and matrix-inclusion interfacial
20 effects [8], [9]. Various bounds of the ETC of composite material have been proposed, such as,
21 based on the rule of mixture, [10], variational principle [11] and statistical correlation functions
22 [12]. These bounds are used to define the thermodynamic limits of the ETC of two-phase
23 composites [2].

1 Several analytical models have been proposed to predict the ETC of a composite material based
2 on simplified microstructures of the composites. Maxwell [13] was one of the first persons to
3 investigate the conduction of two-phase composites analytically by considering the dilute
4 suspension of non-interacting spherical particles. An exact expression for the ETC of composites
5 was obtained by solving the Laplace equation. Maxwell's approach has been extended by many
6 researchers, such as Fricke [14], Nielsen [15], Bruggeman [16], Hamilton and Crosser [17],
7 Benveniste [18] and Hasselman and Johnson [19]. All these modifications extended the
8 applicability of Maxwell's approach for a variety of conditions. However, these models are not
9 applicable to predict the ETC of composites having highly conductive inclusions [3].

10 Many micromechanical models have been proposed to predict the ETC of composites.
11 Benveniste [20] formulated the ETC for multiphase systems by determining the average flux in
12 each constituent. The homogenization was performed using the Mori–Tanaka [21] and a
13 generalized self-consistent model [2]. Verma et al. [22] derived the ETC of two-phase composites
14 containing spherical particles arranged in a three-dimensional cubic geometry. The arrangement
15 was divided into multiple unit cells, and resistor model was used to determine the ETC of the unit
16 cells. All the available micromechanical models in literature offered good predictions of the overall
17 ETC when the V_f was relatively small or when the conductivity of the particle (K_p) was comparable
18 to the conductivity of the matrix (K_m).

19 Various experimental, computational and theoretical studies showed that the ETC of a
20 composite can be significantly altered by the particle shape, size, interfacial thermal resistance
21 aside from volume fraction and K_p/K_m ratio ([2],[23]). Nan et al. [24] developed a generalized
22 effective medium approach (EMA) formulation to compute the ETC of arbitrary ellipsoidal
23 particulate composites with interfacial thermal resistance. The formulation accounted for the effect

1 of particle shape, size, orientation distribution, volume fraction and interfacial thermal resistance.
2 With and without interfacial thermal resistance at a large K_p/K_m ratio, the ETC significantly
3 increases with the anisotropy of the inclusion shape. It was suggested that with large K_p/K_m ratio,
4 the ETC of a composite could be enhanced considerably by reinforcing the matrix with prolate
5 inclusion (e.g., whiskers); while for small K_p/K_m , the spherical particle is suitable to improve
6 ETC.

7 In nano-enhanced composites, the nanoparticles tend to agglomerate during the solid-liquid
8 phase transition. Some studies showed enhancement in ETC with the formation of percolation
9 networks ([25]); while others showed a reduction in ETC ([26]). The percolation threshold
10 depends on the size and the shape of the nanoparticles ([27], [28]). Nan et al. ([24], Gao et al. [29]
11 and Xie et al. [30]) studied the influence of the inclusions on ETC below the percolation threshold
12 while recently Wemhoff [31] developed a percolation threshold model for composite material
13 containing uniformly distributed and oriented cylindrical or prolate inclusion. Along the same line,
14 Wemhoff and Webb [32] studied the influence of both spherical clustering and linear percolation
15 network formation on the ETC of a composite. The EMA and percolation theories were employed
16 for percolated and unpercolated areas. It was shown that both spherical clustering and linear
17 agglomeration tend to reduce the ETC. However, the sensitivity analysis of the model suggested
18 that linear agglomeration can increase bulk thermal conductivity. It was found that when the ratio
19 of inclusion–matrix to inclusion-inclusion Kapitza resistance increases then the relative thermal
20 resistance reduces through the percolation network compared to the unpercolated regions of the
21 domain, which in turn leads to an increase in the ETC of a composite. Recently, Chatterjee et al.
22 [33] proposed a computational heat conduction model based on percolation theory for thermal

1 conductivity of composites with a high volume fraction of filler in the matrix. They considered
2 cubical particle percolation effect to compute the ETC of the composite.

3 Several empirical models have been proposed to predict the ETC of highly thermally
4 conductive composites. Agari and Uno ([3], [4]) and recently by Zhang et al. [34] have shown that
5 at higher V_f and high ratios of particle to matrix thermal conductivity, i.e., $V_f > 15\%$ and K_p/K_m
6 > 100 , a particle interaction in the form of a conductive chain mechanism is exist. This mechanism
7 accelerated the heat conduction process, which was observed due to an increase in the overall ETC
8 of the composite. It was concluded that the V_f and the geometry of the particle were responsible
9 for forming the conductive chain mechanism. Zhou et al. [35] showed that at higher particle
10 concentrations, some particles flocculated to form conductive chains. They introduced the heat
11 transfer passage which took the effect of local concentration fluctuation into account to evaluate
12 the ETC of the composites. Although, Agari and Uno [3] and Zhou et al. [35] models are applicable
13 to predict the ETC of highly conductive composites but the parameters involved in their models
14 need to be determined from the experiments; therefore, these models are rarely used.

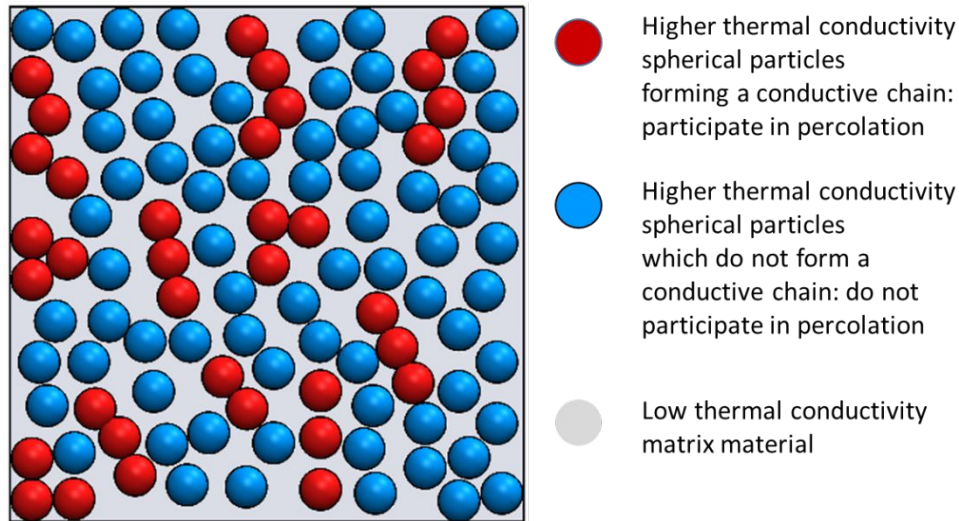
15 The percolation threshold is usually defined in terms of the volume fraction (V_f) and highly
16 dependent on the inclusion geometry. According to the percolation theory [36], the value of the
17 threshold for the cubic particle, V_{fc} , is 0.3117–0.3333. When $V_f < V_{fc}$, the conductive particles are
18 mainly dispersed, and the effect of the particles' interaction on ETC is small. When V_f goes beyond
19 V_{fc} , the connections of the particles increase and the formations of the conductive chains dominate
20 the rise of ETC. Yin et al. [37] mentioned that the threshold limit of percolation could go as high
21 as 0.78. More recently, Liang et al. [28], Gao and Li [38], Wemhoff [31], Wang et al. [27] also
22 observed the dependence of particle size and shape on the percolation threshold.

1 The focus of this study is to present three-dimensional FE percolation models with an attention
2 to find the effect of high conductivity percolation path on the overall ETC of a composite. In this
3 study, FE percolation models were developed purely on thermal conduction physics and analyzed
4 the influence of increasing inclusions' volume fraction on the ETC of the particulate composites
5 numerically. Moreover, for comparison, we have also investigated the 3D micromechanical
6 models based on the conventional spatial distribution of the inclusions, namely, cubical
7 arrangement, hexagonal arrangement, and random distribution. It is emphasized here that there is
8 no study available that explicitly analyze how these conventional 3D micromechanical models will
9 behave at higher volume fractions and the higher mismatch between particle and matrix thermal
10 conductivity. Previously developed micromechanical model and analytical model by the authors
11 for predicting the ETC of two-phase composite were also considered. The comparisons of the
12 proposed models with the experimental data were performed and analyzed.

132. **Details of the proposed percolation model**

14 Agari and Uno [3] demonstrated that with the increase of volume fraction of particles, the chain
15 of the highly conductive particles, i.e., high conductivity percolation paths are formed that
16 drastically increase the ETC of the composite. Percolation is a phenomenon in which the highly
17 conductive particles distributed randomly in the matrix form conductive chains. The inspiration
18 for the geometry of the proposed models comes from the experimental work of Agari and Uno [3]
19 and the percolation theory that is widely used in electrical engineering. We believe that it is worth
20 investigating the role of high conductivity percolation path on the ETC of the particulate
21 composite. The information on the three-dimensional spatial distributions of inclusion are usually
22 not known for the experimental data considered in this study, and generally, the actual
23 microstructure of composite is usually not available in the literature. Therefore, we created

1 percolation models to study the conductive chain mechanism in the particulate composites. The
2 2D Illustration of the typical percolation model considered in this study is shown in Figure 1. The
3 figure clearly shows that the particles (in red) touching each other participate in percolation and
4 accelerate the heat conduction while particles (in blue) which do not form a conductive chain do
5 not participate in percolation.



7 Figure 1: Percolation model showing particles forming a conductive chain and participating in percolation paths, and
8 randomly distributed particles in low thermal conductivity matrix.
9

10 3. Modeling Approach

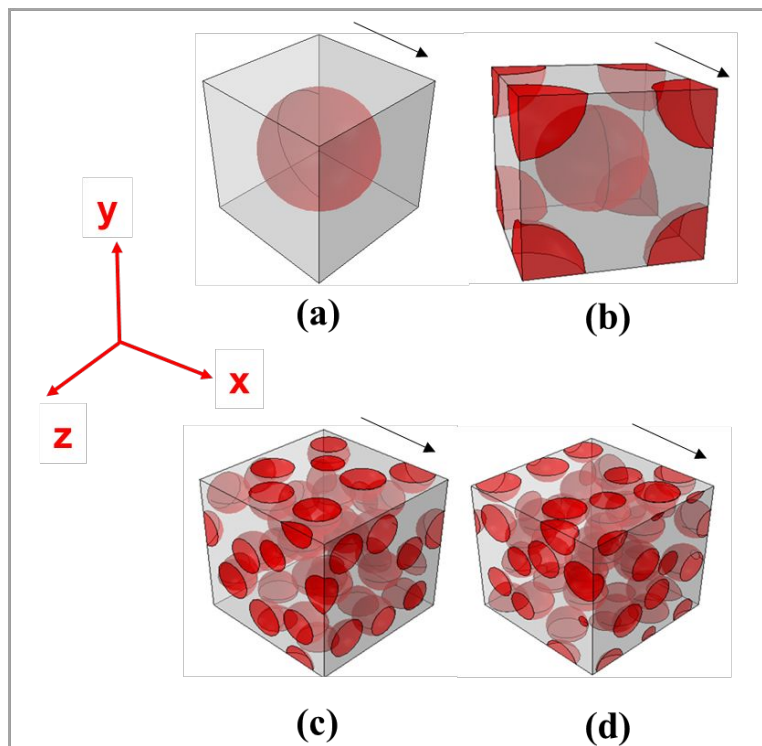
11 Three different modeling approaches are considered, namely, finite element homogenization,
12 micromechanical homogenization, and analytical modeling.

13 3.1. Finite element homogenization

14 3.1.1. Detailed Micromechanical models

15 The thermal conductivity of the particulate composite depends on the microstructural feature of
16 the composite such as the shape, size distribution, spatial distribution, and orientation distribution
17 of the reinforcing inclusions in the matrix [10]. Mostly, real composites possess inclusions with
18 random distributions. The periodic arrangement of the inclusions is usually considered to simplify

1 the problem and acquire insight into the effect of microstructure on the effective properties [39].
2 For example, a particulate composite with a 3D periodic array of particles, an RVE (unit cell)
3 shown in Figure 2(a) and (b) is sufficient to conclude the whole composite [40]. These RVEs are
4 used to study the ETC of particulate composites representing the dilute effects of distribution.
5 On the other hand, RVE with a random distribution of particles is also studied by several
6 researchers [29],[41]. However, the recent experimental studies show that effective thermal
7 properties of the particulate composites increase drastically with highly conductive inclusions in a
8 matrix due to the formation of the conductive chain of particles. The effect of highly conductive
9 inclusion has not been investigated in the literature. In this study, four types of the microstructural
10 arrangements, namely, 3D cubical arrangement, hexagonal arrangement, random distribution, and
11 random network percolation models are considered to investigate their ETC when the ratio of
12 thermal conductivity of particle to the matrix is very high. Figure 2 shows the RVE of these
13 different microstructural arrangements.



14

1 Figure 2 Examples of particulate composite RVE considering detailed microstructural
 2 arrangements of particles at volume fraction 30%, (a) Cubical arrangement. (b) Hexagonal
 3 arrangement, (c) Random distribution, (d) Random network percolation model. The arrow
 4 represents the heat transfer direction.
 5

6 3.1.2. Governing Equation and Constitutive relations

7 For a continuum body with volume, V and surface, S , the thermal equilibrium
 8 governing equation for the temperature field can be defined as [42]:

$$9 \quad q_{i,i} = 0 \quad (1)$$

10 with temperature boundary conditions $\theta = \bar{\theta}$ on Γ_θ and/or heat flux $h_i = q_i n_i = \bar{h}_i$ on Γ_h . Where
 11 $\theta = T - T_0$ is temperature change, T is the absolute current temperature, T_0 is an absolute
 12 reference temperature, h is the normal heat flux, n_i is the outward vector which is normal to the
 13 boundary $\Gamma = \Gamma_\theta \cup \Gamma_h$; \bar{h} and $\bar{\theta}$ are macroscopic heat flux and temperature on the related
 14 boundaries.

15 *Microscopic Constitutive Model*

16 The matrix and particle are assumed to be locally isotropic and homogeneous. The thermal
 17 constitutive law that governs each material or phase in a RVE is given by the Fourier's law of heat
 18 conduction

$$19 \quad q_i = -K_{ij} \varphi_j, \text{ where } \varphi_j = \frac{\partial \theta}{\partial x_j} \quad (2)$$

20 Where, q_i , φ_j and K_{ij} are the components of the heat flux vector, temperature gradient vectors
 21 and the consistent tangent thermal conductivity tensor.

22 *Macroscopic Constitutive Model*

1 The macroscopic constitutive relation is obtained by solving the heat conduction problem on
2 heterogeneous RVE with specified boundary conditions. Based on the imposed boundary
3 conditions, either the macroscopic heat flux or the macroscopic temperature gradient field is
4 calculated by averaging or homogenizing the microscopic counterparts. The effective thermal
5 conductivity is calculated by using the macroscopic constitutive relationships relating the average
6 heat flux ($\overline{q_i}$), and average temperature gradient ($\overline{\varphi_j}$), and is expressed by the Fourier law of heat
7 conduction as:

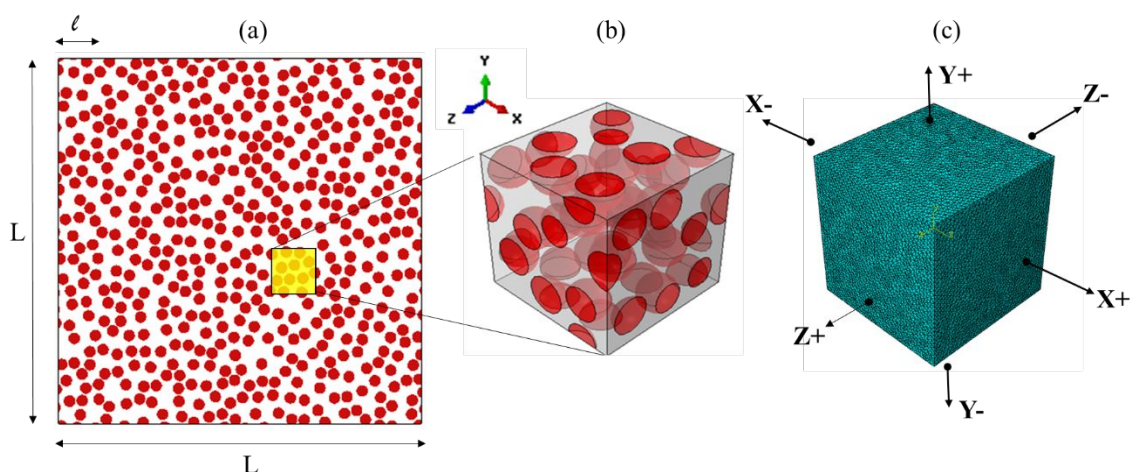
$$8 \quad \overline{q_i} = -\overline{K_{ij}} \overline{\varphi_j}, \text{ where } \overline{\varphi_j} = \frac{\partial \overline{\theta}}{\partial x_j} \quad (3)$$

9 Where $\overline{K_{ij}}$ are the components of the effective thermal conductivity tensor.

10 **3.1.3. Finite Element Models**

11 Finite element models for four types of micromechanical arrangements as shown in Figure 2
12 were generated with a different volume fraction of the particles ranging from 0-50%. The
13 commercial finite element analysis software ABAQUS was used to carry out the heat transfer
14 analysis. RVE's were considered to have highly conductive particles embedded in a low thermal
15 conductivity matrix. The thermal conductivity of the matrix and particles used in this study are
16 given in Table 1. Figure 3 (a) shows the example of the random composite having the macroscopic
17 scale (L) and microscopic scale (l). An example of RVE having a random distribution of particles
18 at 30% volume fractions is shown in Figure 3(b). Meshed RVE with 10-noded quadratic heat
19 transfer elements (DC3D10) showing 6 boundary faces with respect to the axes directions is also
20 shown in Figure 3(c). Each node in the FE model has one degree of freedom of temperature (T).
21 The following assumptions were made in creating the finite element models [43]:

- 1 (1) The characteristic size of the heterogeneities is assumed to be much smaller than the dimension
 2 of an RVE, which in turn is supposed to be small compared to the characteristic length of the
 3 macroscopic structure.
- 4 (2) Both the matrix and the particle phases are homogeneous and isotropic.
- 5 (3) Perfect bonding between the particle and matrix with negligible thermal contact resistance.
- 6 (4) No voids in the matrix and particle.



7
 8 Figure 3 (a) Random distribution of particle (b) RVE (c) Meshed RVE with 10-noded quadratic
 9 heat transfer tetrahedron elements (DC3D10) showing 6 boundary faces with respect to the axes
 10 directions.
 11

12 **Table 1. Thermal conductivity of materials ([3], [4], [7], [5], [44], [6]).**
 13

Material	Thermal Conductivity ($\text{Wm}^{-1} \text{K}^{-1}$)	Material	Thermal Conductivity ($\text{Wm}^{-1} \text{K}^{-1}$)
Polystyrene	0.1549	Silica	1.5
Epoxy	0.195	Alumina	36
High density polyethylene (HDPE)	0.543	Aluminum	204
Polyvinyl chloride	0.1687	Graphite	209.3
CaO (calcium oxide)	15.07	SCAN	220
MgO (magnesium oxide)	54.85		

14
 15
 16 **3.1.4. Boundary conditions**

1 The effective thermal properties of the heterogeneous materials can be determined by applying
 2 four types of boundary conditions [45],[46], to the RVE. The four boundary conditions are listed
 3 here as follows:

4 1. Natural Boundary Condition (NBC)

$$5 \quad h = \bar{q}_i n_i, \quad \langle q_i \rangle = \bar{q}_i, \quad \forall x_i \in \partial B, \quad (4)$$

6 2. Essential Boundary Condition (EBC)

$$7 \quad \theta = \bar{\varphi}_i x_i, \quad \langle \varphi_i \rangle = \bar{\varphi}_i, \quad \forall x_i \in \partial B, \quad (5)$$

8 3. Periodic Boundary Conditions (PBC)

$$9 \quad \begin{aligned} \theta(x_i + L_i) &= \theta(x_i) + \bar{\varphi}_i (x_i^+ - x_i^-), \\ h_i(x_i + L_i) &= -h_i(x_i) \quad \forall x_i \in \partial B, \end{aligned} \quad (6)$$

10 So that $\langle q_i \rangle = \bar{q}_i$, where \bar{q}_i and $\bar{\varphi}_i$ are constant vectors.

11 4. Mixed Boundary Condition (MBC)

$$12 \quad (\theta - \bar{\varphi}_i x_i)(h - \bar{q}_i n_i) = 0, \quad \forall x_i \in \partial B, \quad (7)$$

13 Where, ∂B is the surface boundary of the RVE, n_i is the outer unit normal vector to ∂B , and L is
 14 the length of the periodicity. Generally, for the case of PBC and EBC, $\bar{\varphi}_i$ is applied; while \bar{q}_i is
 15 applied for NBC. In the case of MBC, EBC is applied on one pair of parallel faces, and NBC is
 16 applied on the other pairs. Previous investigations have found that the MBC and PBC are much
 17 more accurate in the micromechanical analysis of composite materials for both periodic materials
 18 and random materials ([47]). Moreover, MBC and PBC yield RVE size independent results while
 19 the results obtained from EBC and NBC converge to those of MBC and PBC as l increases as
 20 shown by [48]. Since cubical and hexagonal arrangements are periodic so PBC can be applied;

1 while MBC should be used for random and percolation models. This study is also utilized MBC
 2 to evaluate effective thermal conductivity due to scale-independence.

3 **3.1.5. Homogenization Method**

4 From the above homogenization procedures, we can see that the flux and temperature on the
 5 boundary of the RVE are sufficient to calculate the effective thermal conductivity of the
 6 composites. The macroscopic heat flux and the macroscopic temperature gradient fields were
 7 computed as the volume averages of the microscopic counterparts, and they were related to each
 8 other by the macroscopic constitutive formulations ([49]).

$$9 \quad \bar{q}_i = \langle q_i \rangle = \frac{1}{V} \int_V q_i dV = \frac{1}{V} \int_{\Gamma} h x_i d\Gamma \quad (8)$$

10

$$11 \quad \bar{\varphi}_i = \langle \varphi \rangle = \frac{1}{V} \int_V \nabla \varphi dV = \frac{1}{V} \int_{\Gamma} \theta n_i d\Gamma \quad (9)$$

12

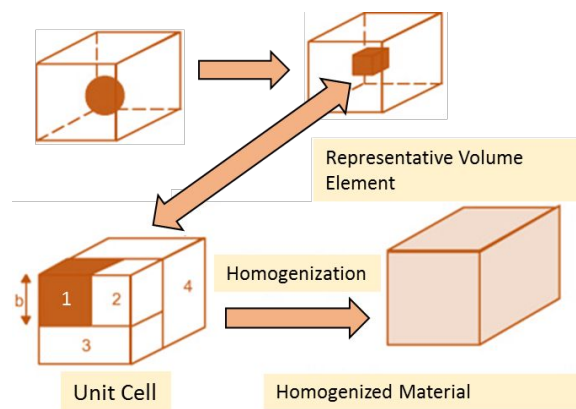
13 Where V is the volume of the RVE. It can be seen from Eq. 8 and 9 that the volume average heat
 14 flux and temperature gradient are related to the flux on the boundary of the RVE.

15 For isotropic case, the ETC tensor can be expressed as $\overline{K}_{ij} = \bar{k} \delta_{ij}$. Thus according to macroscopic
 16 Fourier's law, the ETC can be calculated as $\bar{k} = \|\bar{q}_i\| / \|\bar{\varphi}_i\|$. To eliminate the rate effects and
 17 external influence, all RVE heat transfer simulation should be carried out under steady-state heat
 18 conduction.

19 It is worth mentioning that for highly conductive inclusions, increasing the volume fraction of the
 20 inclusion would cause acceleration in the diffusion process, which cannot be captured by a
 21 Fourier's law of heat conduction presented in Eq. (1) [50]. However, if one neglects size dependent
 22 conduction and assumes steady state conditions, then different diffusion equations will yield the
 23 same effective thermal conductivity for the composite [47].

24 **3.2. Micro-thermal homogenization**

1 Khan and Muliana (2010) developed a micromechanical model for the effective thermal properties
 2 of a particle reinforced composite. In this study, we employed the same model for computing the
 3 effective thermal conductivity of the composite containing highly conductive inclusion in a less
 4 thermally conductive matrix and analyze its suitability. For brevity, we have reviewed the basic
 5 equations describing the ETC formulation. Figure 4 illustrates the simplified micromechanical
 6 model (RVE) for the particulate composite. In the model, a microstructure with the cubical
 7 arrangement of cubic particles in a homogeneous matrix was assumed. A representative volume
 8 element (RVE) with a cubic particle embedded in the center of the matrix with cubic domain. A
 9 one-eighth unit-cell consisting of four sub-cells was modeled due to symmetry. The first sub-cell
 10 was a particle constituent, while subcells 2, 3, and 4 were representing the matrix constituents. The
 11 micromechanical relations gave equivalent homogeneous thermal responses from the
 12 heterogeneous microstructures and simultaneously recognize thermal constitutive behaviors of the
 13 individual constituents. The micromechanical formulations were designed to be compatible with
 14 commercial finite element analyses software, i.e., ABAQUS [1]. In ABAQUS, the effective
 15 responses from the micromechanical relations were implemented at each material point (Gaussian
 16 integration point) within the finite elements as shown in Figure 4.



17

18 **Figure 4 Representative unit-cell model for the particulate composite with cubic particle embedded in a**
 19 **matrix.**

20

1 The micromechanical model was formulated by considering an RVE with a single inclusion
 2 embedded in a cubic matrix. Periodic boundary conditions were imposed on the selected RVE
 3 model. A volume averaging method based on a spatial variation of the temperature gradient in
 4 each subcell was adopted to determine the effective thermal conductivity of the particle reinforced
 5 composites. The average heat flux and temperature gradient are shown here:

$$6 \quad \bar{q}_i = \frac{1}{V} \sum_{m=1}^N \int_{V^{(m)}} q_i^{(m)}(x_k^{(m)}) dV^{(m)} \approx \frac{1}{V} \sum_{m=1}^N V^{(m)} q_i^{(m)} \quad (10)$$

$$7 \quad \bar{\varphi}_i = \frac{1}{V} \sum_{m=1}^N \int_{V^{(m)}} \varphi_i^{(m)}(x_k^{(m)}) dV^{(m)} \approx \frac{1}{V} \sum_{m=1}^N V^{(m)} \varphi_i^{(m)} \quad (11)$$

8
 9
 10 Where N is the total number of sub-cells. The average heat flux within an FE scheme was solved
 11 numerically, and an incremental approach was used to obtain the ETC expression. The incremental
 12 average heat flux can be expressed as:

$$13 \quad d\bar{q}_i = -\bar{K}_{ij} d\bar{\varphi}_j \quad (12)$$

14
 15 The homogenized temperature gradient and heat flux relations are summarized as follows:

$$16 \quad d\bar{\varphi}_i = \frac{1}{V^{(A)}} [V^{(1)} d\varphi_i^{(1)} + V^{(2)} d\varphi_i^{(2)}] = d\varphi_i^{(3)} = d\varphi_i^{(4)} \quad (13)$$

$$17 \quad d\bar{q}_i = \frac{1}{V} [V^{(A)} dq_i^{(A)} + V^{(3)} dq_i^{(3)} + V^{(4)} dq_i^{(4)}] \quad (14)$$

$$18 \quad dq_i^{(A)} = dq_i^{(1)} = dq_i^{(2)} \quad (15)$$

19
 20 Where, the total volume of the subcells 1 and 2 in Eqs. (13) and (14) is $V^{(A)} = V^{(1)} + V^{(2)}$.

21 Let $\mathbf{M}^{(m)}$ be the concentration tensor that relates the average temperature gradient of each
 22 subcell with the overall temperature gradient across the unit cell. The temperature gradient in each
 23 subcell is given by:

$$24 \quad d\varphi_i^{(m)} = M_{ij}^{(m)} d\bar{\varphi}_j \quad (16)$$

25

1 and the incremental form of the heat flux in each subcell is expressed as:

$$2 \quad dq_i^{(m)} = -K_{ij}^{(m)} M_{jk}^{(m)} d\bar{\varphi}_k \quad (17)$$

4 Using Eq. (17), the average incremental heat flux in the unit-cell model is approximated as:

$$5 \quad d\bar{q}_i = -\frac{1}{V} \sum_{m=1}^4 V^{(m)} K_{ij}^{(m)} M_{jk}^{(m)} d\bar{\varphi}_k \quad (18)$$

7 Comparing the above equation with Eq. (12) gives the tangent effective thermal conductivity
8 matrix of the composite, which is:

$$9 \quad \bar{K}_{ik} = -\frac{1}{V} \sum_{m=1}^4 V^{(m)} K_{ij}^{(m)} M_{jk}^{(m)} \quad (19)$$

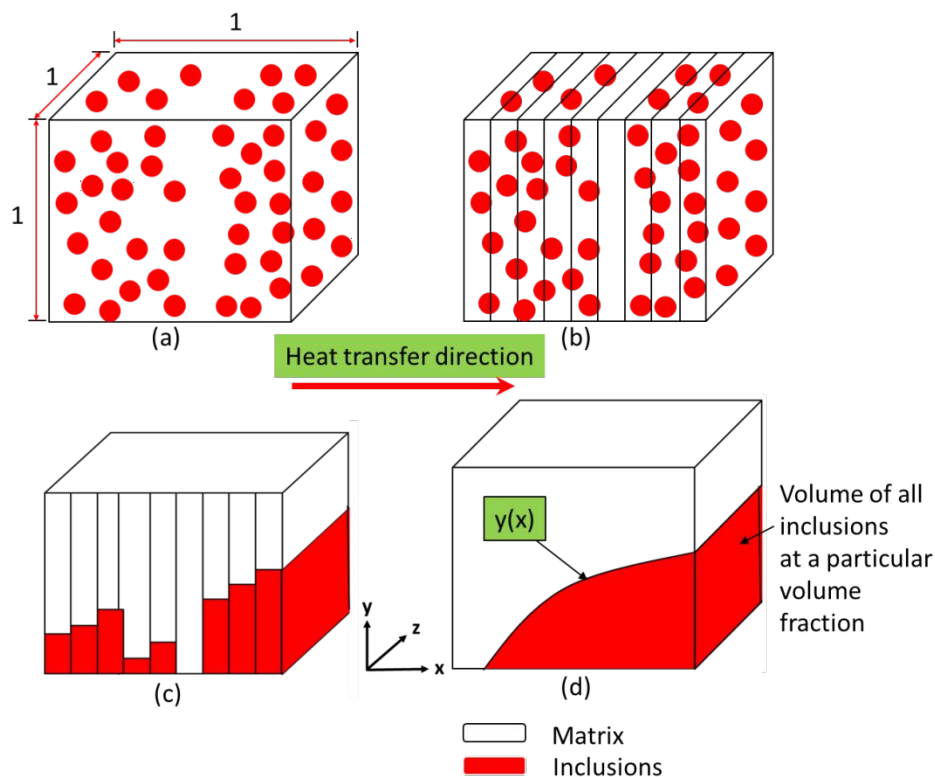
10
11 Detail expression of the $\mathbf{M}^{(m)}$ matrix can be found elsewhere [1].

12 13 **3.3. Analytical Model**

14 Khan et al. [51] proposed an analytical model for ETC of an isotropic two-phase composite
15 material consists of a highly conductive particle as inclusions embedded in a low thermally
16 conductive polymeric matrix. An ideal contact between the inclusions and the matrix was assumed
17 with no porosity in the composite. The ETC expression was derived assuming a unidirectional heat
18 flow, neglecting thermal convection, radiation, and the contact resistance between the matrix and
19 the inclusions. The underlying assumption and procedure to obtain the ETC expression is
20 summarized below.

21 A unit cube (1x1x1) of a two-phase composite material was assumed to have inclusions
22 dispersed in a matrix with some statistical spatial distribution as shown in Figure 5 (a). Some form
23 of continuous distribution of inclusions was usually assumed to determine the analytical
24 expression for the ETC of a composite [52]. The outer surfaces of a cube parallel to xy and xz
25 planes were perfectly insulated, i.e., the direction of heat transfer is along the x-axis. The two-

1 phase composite was hypothetically sliced into numerous thin layers parallel to the yz plane as
 2 shown by the vertical lines in Figure 5 (b). It was assumed that the driving potential (temperature
 3 gradient) for heat conduction in x -direction was uniform through each layer. Each composite layer
 4 had the inclusions and the matrix fractions as shown in Figure 5 (c). Without changing the ETC of
 5 each layer, both inclusions and matrix can equivalently be represented by histograms of matrix
 6 and inclusions to compute the effective resistance of each slice which in turn gives the effective
 7 resistance (ETC) of a unit cell. Alternatively, the sequence of the layers can be re-arranged into a
 8 continuous distribution function of the inclusions to compute the effective resistance of the unit
 9 cell Figure 5 (d). The model obtained was geometrically invariant along the z -axis.



10
 11 **Figure 5. A cubic unit cell for the study of the ETC of a two-phase composite material (after**
 12 **[28]). (a) Inclusions randomly distributed in the matrix, (b) hypothetically sliced thin layers,**
 13 **(c) histogram of the layers and (d) corresponding equivalent continuous distribution of the**
 14 **histogram.**

15

16 The unidirectional effective heat flux (\bar{q}_x) in a unit cube can be expressed as:

$$\bar{q}_x = -k_e \frac{\partial \bar{T}}{\partial x_x} \quad (20)$$

Where, \bar{q}_x is the ETC of a composite and $\partial \bar{T} / \partial x_x$ is the uniform temperature gradient through each layer. For a unit length along the x-axis, the expression for effective resistance (R_e) of a unit cell is given by [52]

$$R_e = \int_0^1 \frac{dx}{k_m + (k_p - k_m)y(x)} + \frac{1-2x}{k_m}; \quad k_e = \frac{1}{R_e} \quad (21)$$

The $y(x)$ is a function that describes the variation in the collective volume of the inclusions (that may vary differently for different distributions) from one V_f to the other V_f of the inclusions. The volume under the surface was formed by the curve projection on xy-plane represents the volume of all inclusions at a particular volume fraction. The ETC (k_e) was obtained from Eq. (21) by taking the inverse of the equivalent overall resistance of the unit cell (R_e) obtained for different distributions. These calculations were only possible if one assumed that the driving potential (temperature gradient) for heat conduction along x-direction was uniform through each layer.

Khan et al. [51] assumed that the sequence of the layers shown in Figure 5(c) can be represented by a linear distribution function of the inclusion material and obtained the following expression for the ETC of a two-phase composite as a function of V_f and the thermal conductivity of the constituents:

$$k_e = \left[\frac{1}{(k_p - k_m)} \ln \left\{ k_m + \sqrt{2V_f} (k_p - k_m) + \sqrt{2V_f} (k_p - k_m) \right\} - \frac{1}{(k_p - k_m)} \ln \left\{ k_m + \sqrt{2V_f} (k_p - k_m) \right\} + \frac{1 - \sqrt{2V_f}}{k_m} \right]^{-1} \quad (22)$$

4.2 Comparison with Other Models

1 4.2.1 Analytical Models

2 To check the efficacy of the proposed model, the predictions were also compared with other
 3 models available in the literature. For brevity, we considered classical models relevant to our study.
 4 Maxwell [13] investigated the conduction of two-phase composites analytically by considering the
 5 dilute suspension of non-interacting spherical particles. An exact expression for the ETC of
 6 composites was obtained by solving the Laplace equation. Jeffrey [53] extended the Maxwell
 7 model and considered the interaction between the pairs of spheres to determine the expression of
 8 ETC of composite and also introduced a parameter that accounts for the role of K_p/K_m ratio on
 9 the ETC. The results were also found to be dependent on how pairs of spheres are distributed with
 10 respect to each other. The ETC expressions for these models are written as follows:

$$11 \quad \text{Maxwell [13]: } k_e = k_m \frac{k_p + 2k_m + 2V_f(k_p - k_m)}{k_p + 2k_m - V_f(k_p - k_m)} \quad (23)$$

12

$$13 \quad \text{Jeffrey [53]: } k_e = k_m + 3k_m V_f \left[1 + V_f \frac{\sigma_1(2k_m + k_p) + (k_p - k_m)}{2k_m + k_p} \right] \frac{(k_p - k_m)}{2k_m + k_p} \quad (24)$$

14

15 σ_1 is parameter depending on the thermal conductivity ratio.

16 4.2.2 Numerical Models

17 Several numerical models are also available to determine the ETC of particulate composites.
 18 For example, ETC of random two-phase composite materials was obtained by considering the
 19 shape, spatial distribution, thermal contact resistance, and particles V_f ([23],[54],[39] and
 20 references therein). Experimental and numerical ETC of polymer matrix filled with metallic
 21 spheres were presented by Karki et al. ([41]). The effects of the filler concentrations, the ratio of
 22 thermal conductivities of filler to the matrix material and the Kapitza resistance of the contact

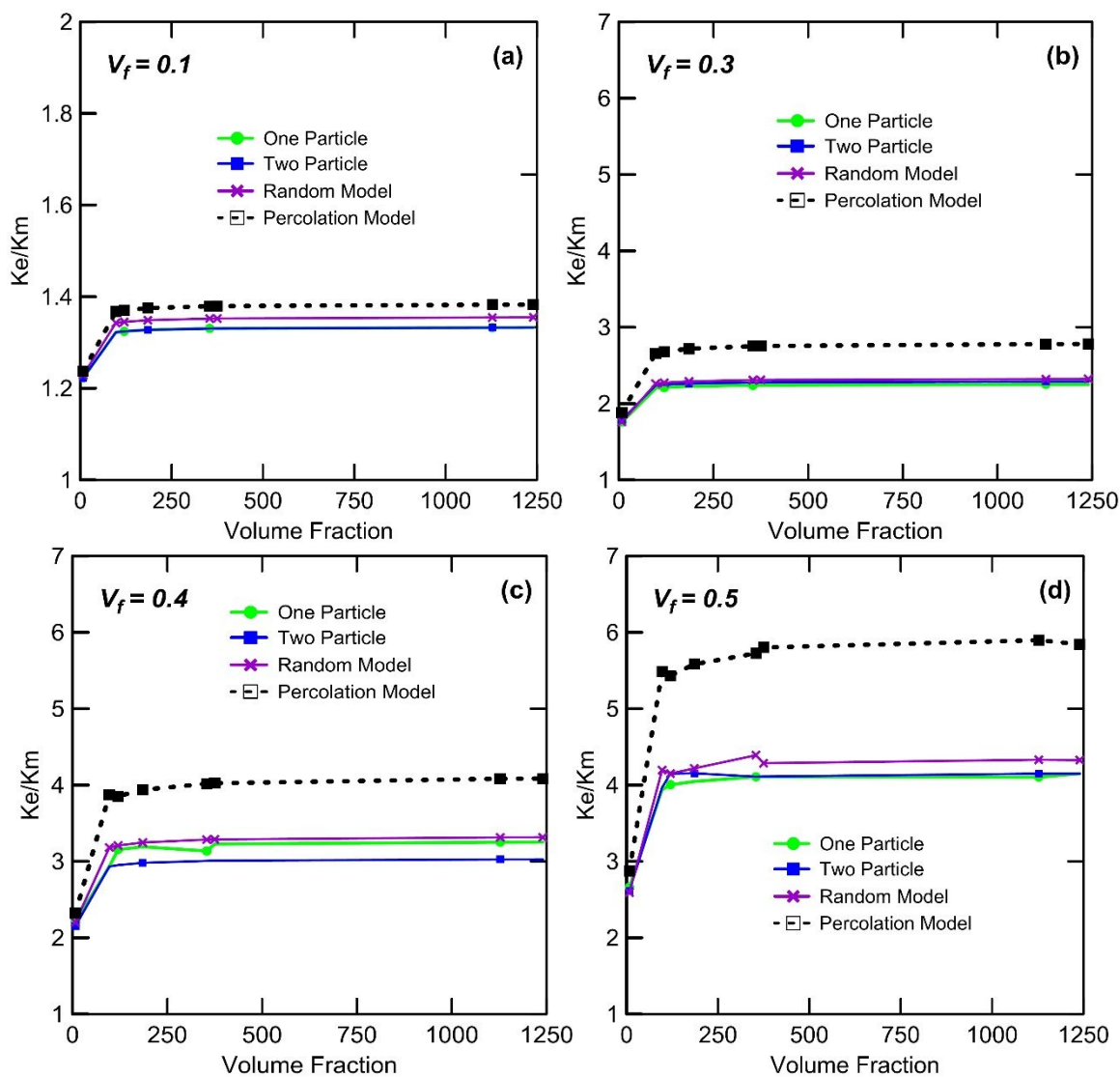
1 inclusion/matrix on the ETC were investigated. For more details and updated review/references
2 on the numerical modeling of the ETC of particulate composites, please see [41]. To the best
3 knowledge of the authors, there is only one model available in the literature that considered the
4 effect of the embedding highly conductive inclusions in a less thermally conductive matrix on the
5 ETC of particulate composites. Zhang et al. [34] proposed a randomly mixed model to compute
6 the ETC of particulate composites numerically with respect to the V_f of the particles and the ratio
7 of the thermal conductivity of the particle to that of the matrix. The cubic shape particles of uniform
8 size were generated randomly using a computer program. The steady state heat equation was
9 solved by the finite difference method directly for the composite with appropriate boundary
10 conditions.

11 12 **4. Results and Discussion**

13 Results obtained from the proposed finite element homogenization, analytical solutions, and
14 micromechanical models were compared with already published experimental data and other
15 models in literature which were developed explicitly for highly conductive particulate composites.

16 We investigated the effect of conductivity mismatch on the ETC of the particulate composites.
17 The effect of the different distribution of the inclusions were analyzed, and four RVE of proposed
18 micromechanical models with detailed microstructure were considered. Figure 6 shows how the
19 ETC of composite increases with respect to the matrix conductivity with the increase of the
20 conductivity mismatch (K_p/K_m ratio). It was found that one particle model showed the lowest
21 increase in the overall thermal conductivity while the percolation model showed the highest values.
22 At lower volume fraction there was not a significant difference in the increase of the ETC for all
23 models. However, as the volume fraction was increased beyond 0.3, then the ETC of the
24 percolation models was increased with respect to the matrix material conductivity. As per the

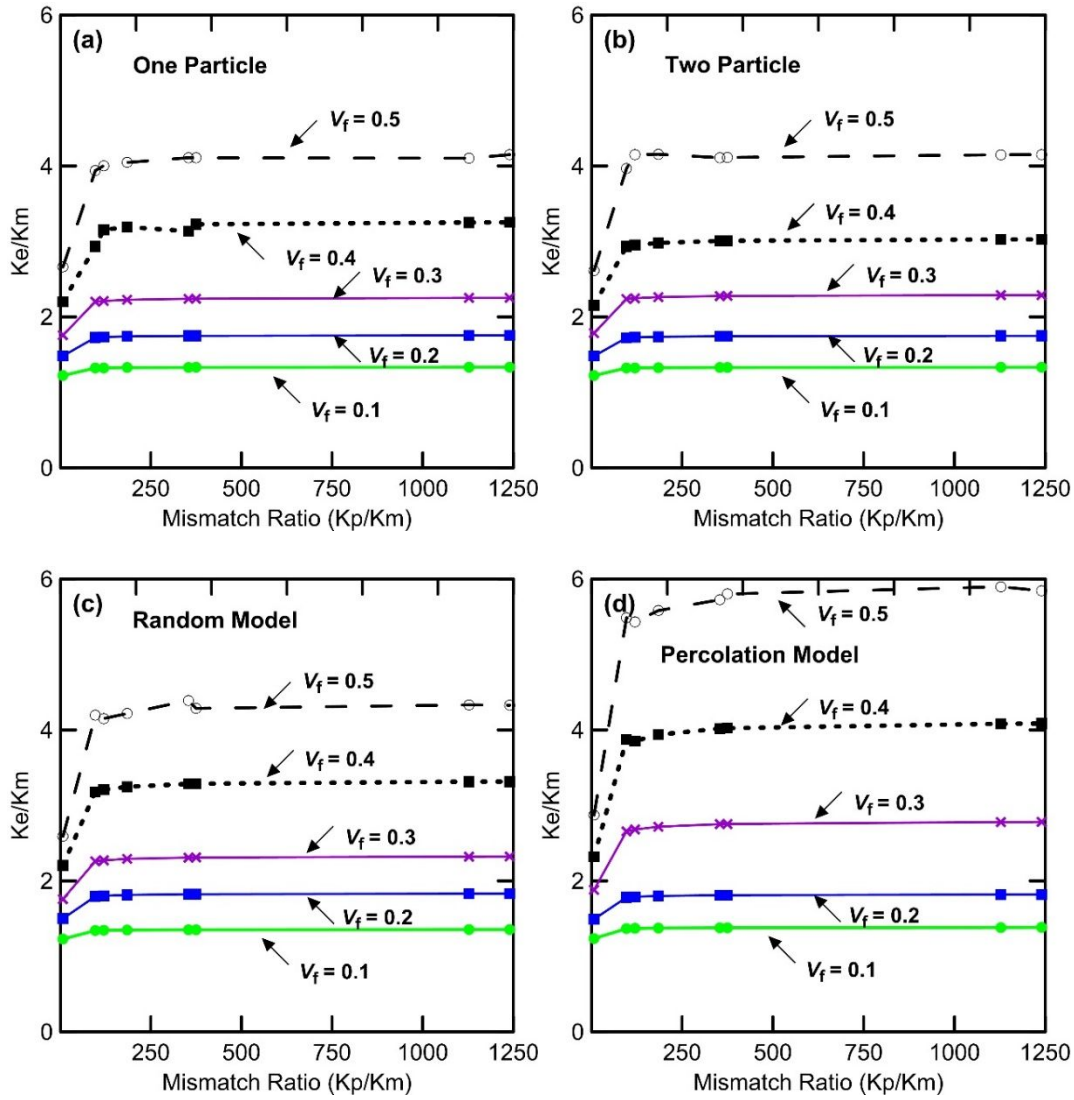
1 percolation theory [36], after V_{fc} beyond 0.3, the particles were increased, and the formations of
 2 the conductive chains thus played a dominant role in the increase of ETC.



5 Figure 6. Conductivity mismatch in a two-phase composite material and its effect on the ETC for various
 6 micromechanical models..

7
 8 For completeness, we studied the conductivity mismatch effect on the ETC for all proposed
 9 models. Figure 7 shows the result of conductivity mismatch at different volume fraction for each
 10 model. It was found that among all the models considered the linear model produced the highest
 11 increase in the ETC with respect to the matrix material thermal conductivity. The simplified
 12 micromechanical model showed the lowest increase in the ETC. One particle, two particles, and

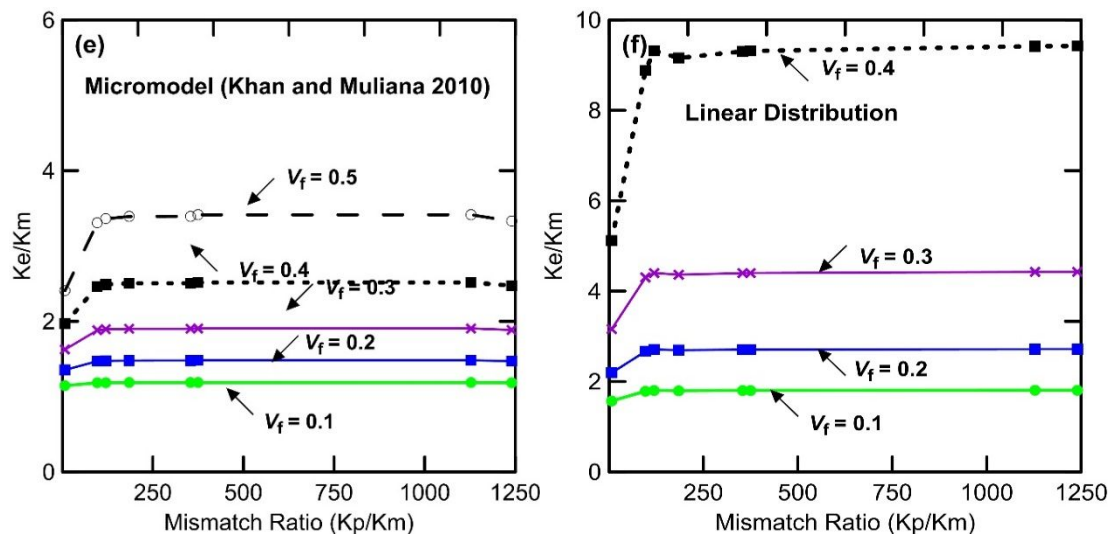
- 1 random particle model showed a similar trend in the increase of the ETC with respect to the matrix
- 2 material.



3

4

5



1
2 Figure 7. Conductivity mismatch in a two-phase composite material and its effect on the ETC for various
3 micromechanical models.

4
5 Figure 8 was used to analyze the percent increase in the ETC that was obtained with respect to the
6 matrix materials. Again the maximum ETC was predicted using the linear model. As a comparison,
7 we showed the results at two volume fraction for all models. We observed that at $V_f = 0.1$, almost
8 all the micromechanical models yielded very low values except the linear model which gave nearly
9 80% higher ETC values than the matrix conductivity. While at $V_f = 0.3$, the linear model provided
10 350% higher than the matrix conductivity as compared to the percolation model which yielded
11 180% higher than the matrix conductivity.

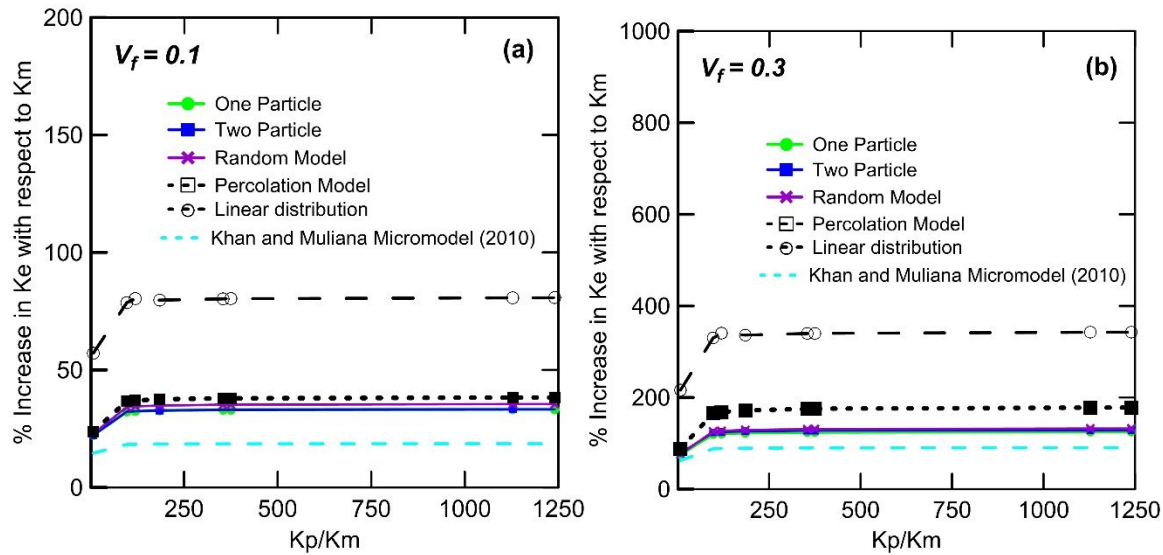
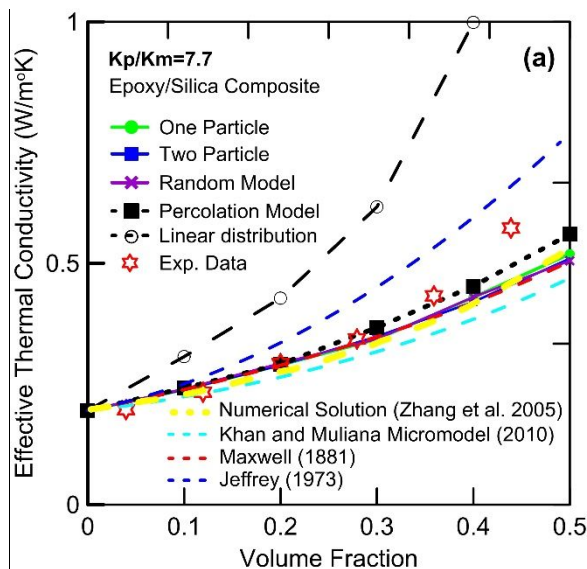


Figure 8. Conductivity mismatch in a two-phase composite material and its effect on the ETC for various micromechanical models.

4.1 Comparison with Experimental Data

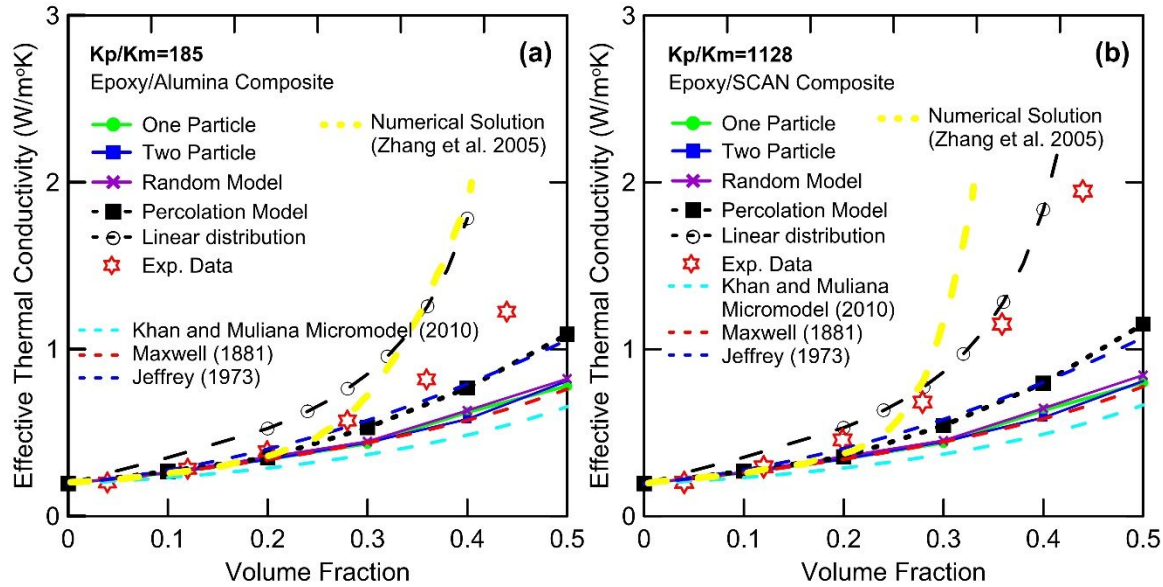
The ETC of epoxy filled with silica ($K_p/K_m=7.7$), alumina ($K_p/K_m=185$) and silica-coated aluminum nitride (SCAN, $K_p/K_m=1128$) particulates was experimentally studied by Wong and Bolampally [7]. The average particle size of the fillers used was 12–15 microns. The thermal conductivities of all materials used in this study are given in Table 1. Figure 9 showed the comparisons of the experimental and predicted ETC for ratio $K_p/K_m=7.7$. For all K_p/K_m , the models observed with reasonable estimates but linear and Jeffrey models overestimated the ETC.



1
2 Figure 9. Conductivity mismatch in a two-phase composite material and its effect on the ETC for various
3 micromechanical models.
4

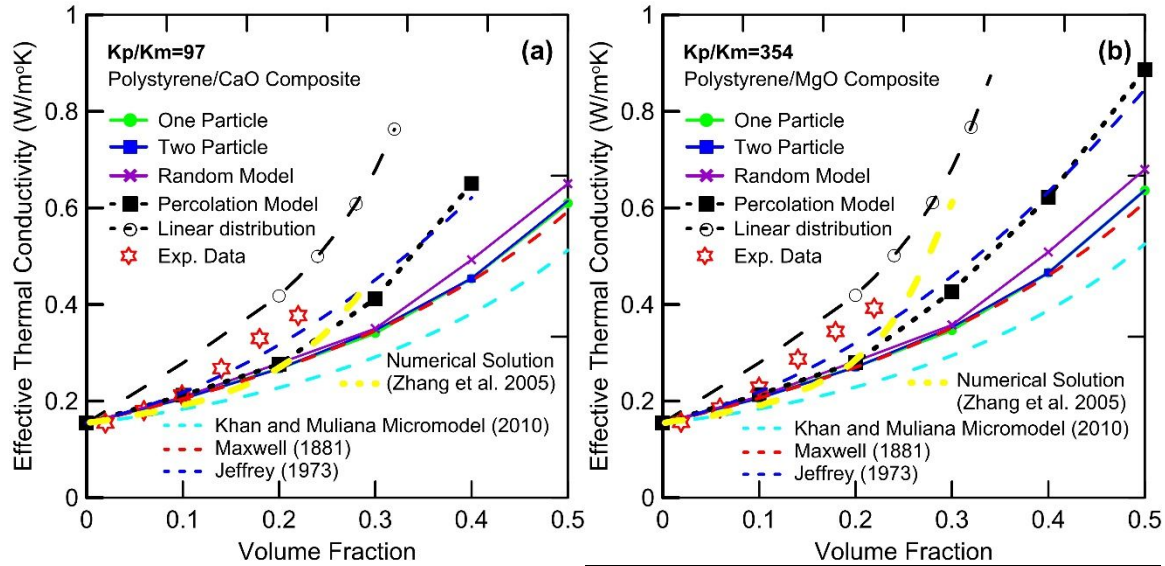
5 The comparison of the experimental, the predicted ETC of epoxy filled with alumina
6 ($K_p/K_m=185$) and silica-coated aluminum nitride (SCAN, $K_p/K_m=1128$) particulates with
7 different models are shown in Figure 10. For, $K_p/K_m=185$, the percolation model and Jeffrey
8 model were observed with reasonable estimation. Maxwell model, micromechanical model, one
9 particle, two particles, and random model were found with reasonable estimates until $V_f < 20\%$.
10 They showed an underestimation of the ETC at higher V_f . The linear model and numerical solution
11 overestimated the ETC, but after $V_f > 30\%$ both models showed a similar trend of increase in the
12 ETC with the increase of V_f . For $K_p/K_m=1128$, all the models deviated from the experimental data
13 after $V_f > 20\%$; while linear distribution gave acceptable estimates. The numerical model was
14 observed with a reasonable estimate until $V_f < 30\%$, and after that, the results have deviated
15 significantly.

16
17
18



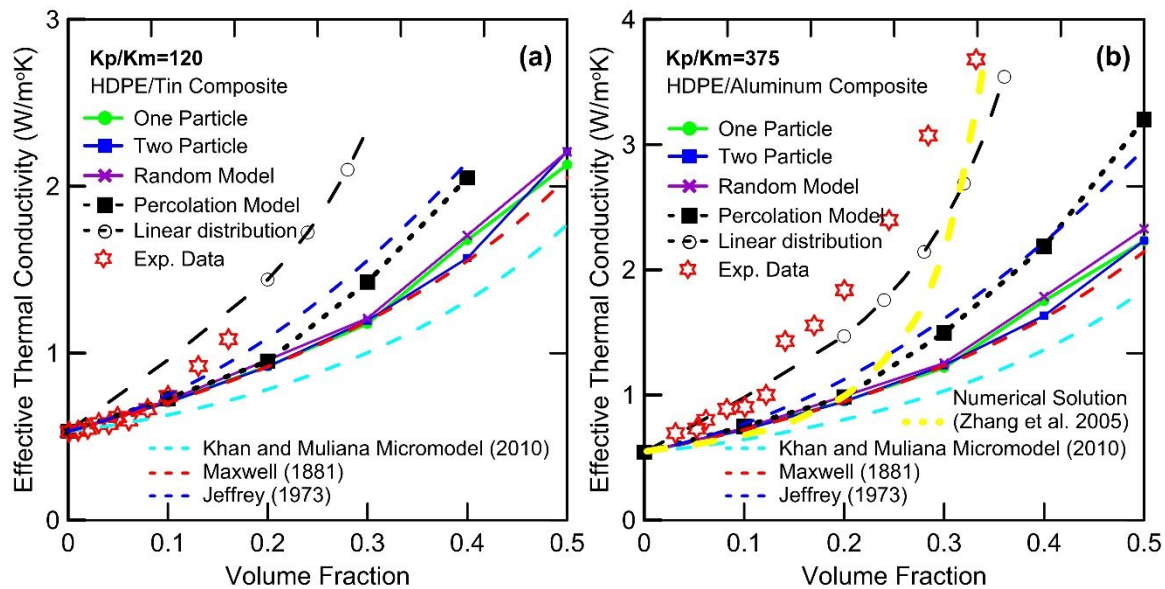
1
2 **Figure 10. Comparison of the experimental data and predicted ETC for a) Epoxy/Alumina**
3 **b) Epoxy/silica coated aluminum nitride composites.**
4
5

6 Comparison of the experimental data and the predicted ETC of polystyrene filled with CaO
7 ($K_p/K_m=97$) and MgO ($K_p/K_m=354$) particulates are presented in Figure 11. The experimental
8 data were obtained by Sundstrom and Lee [5]. The calcium oxide and magnesium oxide were
9 powders with particles approximately spherical in shape and particle size in the range of 62-125
10 microns. For both cases, the Jeffrey model observed with the best estimates of the ETC. Both the
11 numerical model and percolation model were providing a consistent trend of increase in the ETC
12 with the increase of V_f . Maxwell model, micromechanical model, one particle, two particles, and
13 random model were observed with reasonable estimates until $V_f < 10\%$; but they were providing
14 underestimated values of the ETC at higher V_f . In both cases, the linear model overestimated the
15 ETC as compared to all the other models.
16



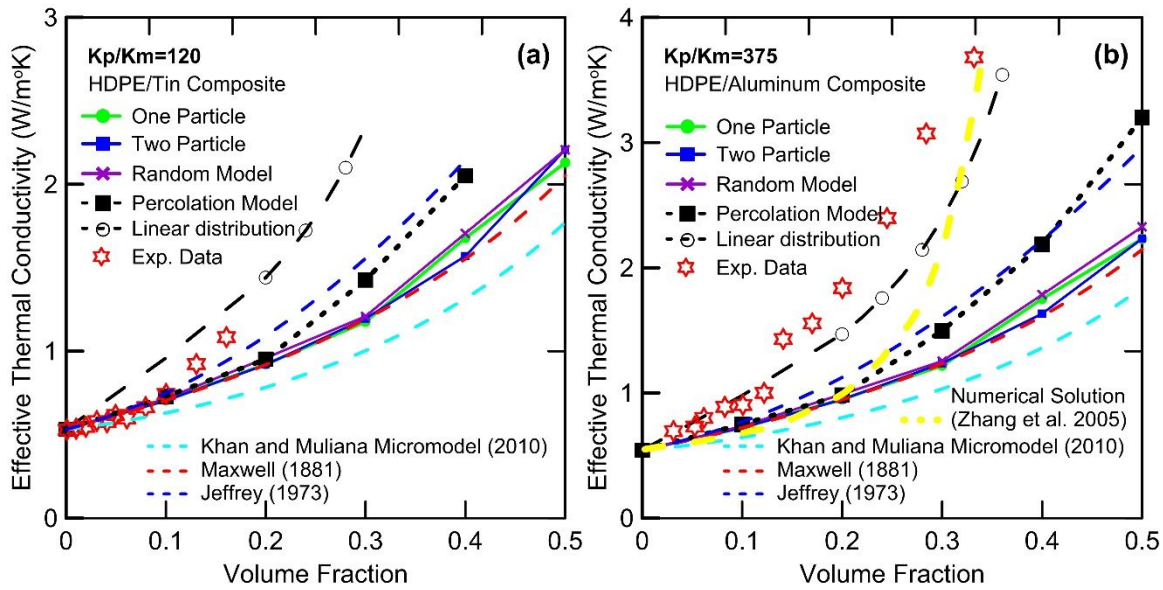
1
2 **Figure 11. Comparison of the experimental data and predicted ETC for a)**
3 **Polystyrene/CaO b) Polystyrene/MgO composites.**

4
5 Kumlutas et al. [44] and Tavman [6] experimentally studied the ETC of high-density
6 polyethylene filled with tin ($K_p/K_m=120$) and aluminum ($K_p/K_m=375$) inclusions. The metallic
7 fillers of tin and aluminum used in the form of fine powder with particles approximately spherical
8 in shape and particle size in the range of 20–40 and 40–80 microns, respectively. The comparison
9 of the experimental data and the predicted ETC with different models are shown in Figure 12



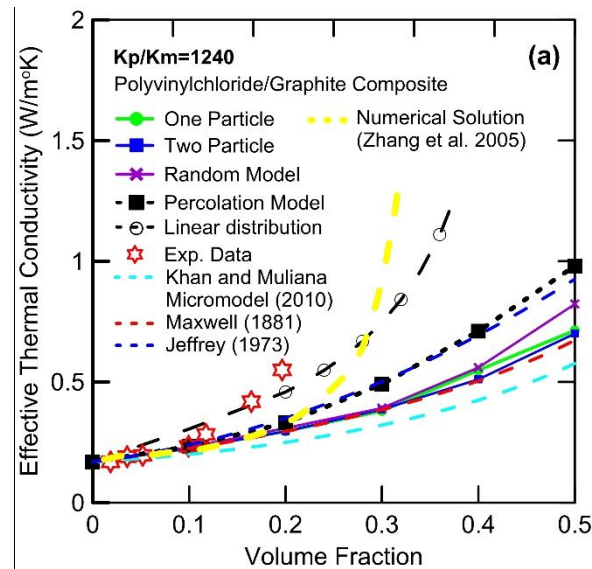
10

1 Figure 12. For $K_p/K_m=120$, Jeffrey and percolation model were with the best estimates and
 2 provided trends in the increase of ETC. All other models underestimated the predictions except
 3 the linear model. However, for $K_p/K_m=375$, linear distribution was observed with quite reasonable
 4 estimates of the trend in the increase of ETC with the increase of V_f of the inclusions. However,
 5 all other models underestimated the ETC at this ratio.



7
 8 **Figure 12. Comparison of the experimental data and predicted ETC for a)**
 9 **HDPE/Aluminum b) HDPE/Tin composites.**

10
 11 Agari and Uno ([3], [4]) studied Graphite based composites and observed that at higher V_f the
 12 graphite flakes agglomerated and formed the conductive chain and as a result ETC of the
 13 composite was considered to increase drastically [24]. The average particle size of the fillers used
 14 was 44–149 microns. Figure 13 shows the comparison of the experimental data and the predicted
 15 ETC. The linear distribution provided the best estimates. Jeffrey and percolation models provided
 16 a reasonable estimate and showed the same tendency as the experimental data. All other models
 17 underestimated the ETC. The results covered the commonly used range of the thermal conductivity
 18 ratio of matrix to the inclusions, i.e., $K_p/K_m=10 - 1240$.



1
2 **Figure 13. Comparison of the experimental data and predicted ETC for a)**
3 **Polyvinylchloride/Graphite b) Polyethylene/Graphite composites.**

4
5 **4.2 Discussion**

6 It can be realized that for all the available experimental data, the trend shows an increase of
7 ETC with the increase of V_f of the inclusions. All analytical models show good predictions of the
8 overall ETC when the V_f is relatively small, but the predictions tend to deviate as the V_f increases.
9 However, in most of the analyzed cases, linear distribution, Jeffrey and Percolation models
10 effectively predict the trend in the increase of ETC with the increase of V_f of the inclusions.

11 If we recall the assumption of Maxwell's equation: there is no interaction among the particles.
12 Jeffrey [53] extended the Maxwell model and considered the interaction between the pairs of
13 spheres to determine the expression of ETC of the composite. On the other hand, an analytical
14 model is based on the linear distribution of the dispersed particles which effectively considered
15 the interaction between the pairs of spheres to determine the expression for the ETC of a two-
16 phase composite as a function of V_f and the thermal conductivity of the constituents. The
17 micromechanical model computes the ETC based on the unit cell representing a dilute suspension

1 of non-interacting spherical particles. The possibility of the explicit formation of particle chains is
2 not considered in all these models.

3 Since we used the Digimat software to create the FE percolation models, so we do not have enough
4 control over the algorithm of particle generation. The software gives us FE models with limited
5 percolation effects, for example, a maximum of 20-30 percolated chains are usually formed
6 depending on the volume fraction. After investigating the location of spheres, it was found that the
7 chain of the highly conductive particles, i.e., high conductivity percolation paths, consists of
8 maximum 4 spheres touching each other (2D Illustration is shown in Figure 1). This limited chain
9 length was found insufficient in getting the enhancement of the ETC, and it was the primary reason
10 for significant differences between estimated and experimental ETC at higher volume fractions
11 and the higher mismatch between particle and matrix thermal conductivity. However, the
12 percolation models were found competitive in describing the sphere interaction mechanism and
13 almost reproduces the results of Jeffrey's model [53].

14 We observed that the proposed analytical model with linear distribution worked very well for
15 most of the particulate composites. For such highly conductive composites, we recommended that
16 experiments should be performed to find the real 3D spatial distribution and connectivity of the
17 inclusions. We plan to conduct experiments by ourselves to acquire the 3D spatial distribution of
18 the clusters and conductive chains of particles using micro CT to generate real microstructure of
19 particulate composites. Nevertheless, we still believed that the percolation modeling approach
20 could be used to predict the ETC of particulate composites provided several long conductive chains
21 should connect the opposite faces of the matrix, which is not the case in the proposed model due
22 to software limitations. To resolve this issue, we also plan to develop our algorithm to generate

1 spatially controlled and architected chains of spheres to study their effect on the ETC of the
2 particulate composites.

3 It should be realized that the discrepancies in predictions in comparison with the experimental
4 data are due to a number of other reasons: 1- The model does not account for the effect of particle
5 shape, 2- size, orientation distribution, interfacial thermal resistance and the effect on particle
6 agglomeration on the enhancement of the ETC of a composite were not considered. For such work,
7 we refer to the work of Nan et al. [24], Prasher et al. [25], Hong et al. [55] and more recently by
8 Wemhoff [31] and Wemhoff & Webb [32].

9

10 **4. Conclusions**

11 Two micromechanical modeling approaches were presented to predict the ETC of two-phase
12 composites containing inclusions with very high thermal conductivity than the matrix. The first
13 modeling approach introduced four micromechanical models based on the various spatial
14 distribution. Finite element homogenization was performed to compute the ETC. In the second
15 approach, a simplified micromechanical model with one particle embedded in a matrix was
16 considered. The micromechanical model used four particle and matrix subcells. Micromechanical
17 relations were formulated in terms of incremental average heat flux and temperature gradient, in
18 the subcells. The first order homogenization scheme was applied, and ETC was formulated by
19 imposing heat flux and temperature continuity at the subcells' interfaces. The predictions obtained
20 from both modeling approaches were compared with the published experimental data and other
21 models available in the literature. It was found that the random network percolation models gave
22 reasonable estimates and showed a rational trend in the increase of ETC for the high K_p/K_m ratio
23 as compared to the ones obtained from the other micromechanical models.

1 Moreover, it was found that the analytical solution based on the linear distribution of the
2 inclusions provided reasonable estimates with the increase of ETC for the high K_p/K_m ratio. We
3 concluded that conductive chain mechanism could be adequately represented by the
4 micromechanical model based on random network percolation models and Jeffrey model in which
5 the inclusions were distributed randomly in a matrix but form limited connections and interaction
6 among inclusions. It was also concluded that with further improvement of the percolation models
7 such as introducing more conductive particle chains and use of smaller size particles with
8 clustering effects may improve the prediction of the ETC.

9

1 **REFERENCES**

- 2 [1] K. A. Khan and A. H. Muliana, "Effective thermal properties of viscoelastic composites
3 having field-dependent constituent properties," *Acta Mech.*, vol. 209, no. 1–2, pp. 153–178,
4 2010.
- 5 [2] S. Torquato, *Random heterogeneous materials: microstructure and macroscopic
6 properties*, vol. 16. Springer Science & Business Media, 2013.
- 7 [3] Y. Agari and T. Uno, "Thermal conductivity of polymer filled with carbon materials: Effect
8 of conductive particle chains on thermal conductivity," *J. Appl. Polym. Sci.*, vol. 30, no. 5,
9 pp. 2225–2235, May 1985.
- 10 [4] Y. Agari and T. Uno, "Estimation on thermal conductivities of filled polymers," *J. Appl.
11 Polym. Sci.*, vol. 32, no. 7, pp. 5705–5712, Nov. 1986.
- 12 [5] D. W. Sundstrom and Y.-D. Lee, "Thermal conductivity of polymers filled with particulate
13 solids," *J. Appl. Polym. Sci.*, vol. 16, no. 12, pp. 3159–3167, 1972.
- 14 [6] I. H. Tavman, "Effective thermal conductivity of isotropic polymer composites," *Int.
15 Commun. Heat Mass Transf.*, vol. 25, no. 5, pp. 723–732, 1998.
- 16 [7] C. P. Wong and R. S. Bollampally, "Thermal conductivity, elastic modulus, and coefficient
17 of thermal expansion of polymer composites filled with ceramic particles for electronic
18 packaging," *J. Appl. Polym. Sci.*, vol. 74, no. 14, pp. 3396–3403, 1999.
- 19 [8] R. C. Progelhof, J. L. Throne, and R. R. Ruetsch, "Methods for predicting the thermal
20 conductivity of composite systems: a review," *Polym. Eng. Sci.*, vol. 16, no. 9, pp. 615–
21 625, 1976.
- 22 [9] D. W. Abueidda, R. K. Abu Al-Rub, A. S. Dalaq, D.-W. Lee, K. A. Khan, and I. Jasiuk,
23 "Effective conductivities and elastic moduli of novel foams with triply periodic minimal
24 surfaces," *Mech. Mater.*, vol. 95, pp. 102–115, Apr. 2016.
- 25 [10] S. Nemat-Nasser and M. Hori, *Micromechanics: overall properties of heterogeneous
26 materials*. Elsevier, 2013.
- 27 [11] Z. Hashin and S. Shtrikman, "A variational approach to the theory of the elastic behaviour
28 of polycrystals," *J. Mech. Phys. Solids*, vol. 10, no. 4, pp. 343–352, 1962.
- 29 [12] T. C. Lim, "Unified practical bounds for the thermal conductivity of composite materials,"
30 *Mater. Lett.*, vol. 54, no. 2, pp. 152–157, 2002.
- 31 [13] J. C. Maxwell, *A treatise on electricity and magnetism*, vol. 1. Clarendon press, 1881.
- 32 [14] H. Fricke, "The Maxwell-Wagner Dispersion in a Suspension of Ellipsoids," *J. Phys.
33 Chem.*, vol. 57, no. 9, pp. 934–937, Sep. 1953.
- 34 [15] L. E. Nielsen, *Predicting the Properties of Mixtures: Mixture Rules in Science and
35 Engineering, 1978*. Marcel Dekker, New York.
- 36 [16] D. A. G. Bruggeman, "The prediction of the thermal conductivity of heterogeneous
37 mixtures," *Ann Phys*, vol. 24, pp. 636–664, 1935.
- 38 [17] R. L. Hamilton and O. K. Crosser, "Thermal Conductivity of Heterogeneous Two-
39 Component Systems," *Ind. Eng. Chem. Fundam.*, vol. 1, no. 3, pp. 187–191, Aug. 1962.
- 40 [18] Y. Benveniste, "On the effective thermal conductivity of multiphase composites," *Z. Für
41 Angew. Math. Phys. ZAMP*, vol. 37, no. 5, pp. 696–713, Sep. 1986.
- 42 [19] D. P. H. Hasselman and L. F. Johnson, "Effective Thermal Conductivity of Composites
43 with Interfacial Thermal Barrier Resistance," *J. Compos. Mater.*, vol. 21, no. 6, pp. 508–
44 515, Jun. 1987.

- 1 [20] Y. Benveniste, "Effective thermal conductivity of composites with a thermal contact
2 resistance between the constituents: Nondilute case," *J. Appl. Phys.*, vol. 61, no. 8, pp.
3 2840–2843, Apr. 1987.
- 4 [21] T. Mori and K. Tanaka, "Average stress in matrix and average elastic energy of materials
5 with misfitting inclusions," *Acta Metall.*, vol. 21, no. 5, pp. 571–574, 1973.
- 6 [22] L. S. Verma, A. K. Shrotriya, R. Singh, and D. R. Chaudhary, "Thermal conduction in two-
7 phase materials with spherical and non-spherical inclusions," *J. Phys. Appl. Phys.*, vol. 24,
8 no. 10, p. 1729, 1991.
- 9 [23] M. Aadmi, M. Karkri, L. Ibos, and M. E. Hammouti, "Effective thermal conductivity of
10 random two-phase composites," *J. Reinf. Plast. Compos.*, vol. 33, no. 1, pp. 69–80, 2014.
- 11 [24] C.-W. Nan, R. Birringer, D. R. Clarke, and H. Gleiter, "Effective thermal conductivity of
12 particulate composites with interfacial thermal resistance," *J. Appl. Phys.*, vol. 81, no. 10,
13 pp. 6692–6699, May 1997.
- 14 [25] R. Prasher, W. Evans, P. Meakin, J. Fish, P. Phelan, and P. Keblinski, "Effect of
15 aggregation on thermal conduction in colloidal nanofluids," *Appl. Phys. Lett.*, vol. 89, no.
16 14, p. 143119, Oct. 2006.
- 17 [26] R. Ehid, R. D. Weinstein, and A. S. Fleischer, "The shape stabilization of paraffin phase
18 change material to reduce graphite nanofiber settling during the phase change process,"
19 *Energy Convers. Manag.*, vol. 57, pp. 60–67, May 2012.
- 20 [27] Y. Wang, G. J. Weng, S. A. Meguid, and A. M. Hamouda, "A continuum model with a
21 percolation threshold and tunneling-assisted interfacial conductivity for carbon nanotube-
22 based nanocomposites," *J. Appl. Phys.*, vol. 115, no. 19, p. 193706, May 2014.
- 23 [28] L. H. Liang, Y. G. Wei, and B. Li, "Thermal conductivity of composites with nanoscale
24 inclusions and size-dependent percolation," *J. Phys. Condens. Matter*, vol. 20, no. 36, p.
25 365201, 2008.
- 26 [29] L. Gao, X. Zhou, and Y. Ding, "Effective thermal and electrical conductivity of carbon
27 nanotube composites," *Chem. Phys. Lett.*, vol. 434, no. 4–6, pp. 297–300, Feb. 2007.
- 28 [30] S. H. Xie, Y. Y. Liu, and J. Y. Li, "Comparison of the effective conductivity between
29 composites reinforced by graphene nanosheets and carbon nanotubes," *Appl. Phys. Lett.*,
30 vol. 92, no. 24, p. 243121, Jun. 2008.
- 31 [31] A. P. Wemhoff, "Thermal conductivity predictions of composites containing percolated
32 networks of uniform cylindrical inclusions," *Int. J. Heat Mass Transf.*, vol. 62, pp. 255–
33 262, Jul. 2013.
- 34 [32] A. P. Wemhoff and A. J. Webb, "Investigation of nanoparticle agglomeration on the
35 effective thermal conductivity of a composite material," *Int. J. Heat Mass Transf.*, vol. 97,
36 pp. 432–438, Jun. 2016.
- 37 [33] A. Chatterjee, R. Verma, H. P. Umashankar, S. Kasthuriengan, N. C. Shivaprakash, and U.
38 Behera, "Heat conduction model based on percolation theory for thermal conductivity of
39 composites with high volume fraction of filler in base matrix," *Int. J. Therm. Sci.*, vol. 136,
40 pp. 389–395, 2019.
- 41 [34] H. Zhang, X. Ge, and H. Ye, "Effectiveness of the heat conduction reinforcement of
42 particle filled composites," *Model. Simul. Mater. Sci. Eng.*, vol. 13, no. 3, p. 401, 2005.
- 43 [35] H. Zhou, S. Zhang, and M. Yang, "The effect of heat-transfer passages on the effective
44 thermal conductivity of high filler loading composite materials," *Compos. Sci. Technol.*,
45 vol. 67, no. 6, pp. 1035–1040, 2007.
- 46 [36] D. Stauffer and A. Aharony, *Introduction To Percolation Theory*. CRC Press, 1994.

- 1 [37] H. M. Yin, G. H. Paulino, W. G. Buttlar, and L. Z. Sun, "Effective thermal conductivity of
2 two-phase functionally graded particulate composites," *J. Appl. Phys.*, vol. 98, no. 6, p.
3 063704, Sep. 2005.
- 4 [38] L. Gao and Z. Li, "Effective medium approximation for two-component nonlinear
5 composites with shape distribution," *J. Phys. Condens. Matter*, vol. 15, no. 25, p. 4397,
6 2003.
- 7 [39] K. A. Khan, R. Barello, A. H. Muliana, and M. Lévesque, "Coupled heat conduction and
8 thermal stress analyses in particulate composites," *Mech. Mater.*, vol. 43, no. 10, pp. 608–
9 625, 2011.
- 10 [40] R. S. Choudhry, Kamran A. Khan, Sohaib Zia Khan, Muhammad Ali Khan, Abid Hassan,
11 "Micromechanical Modeling of 8-Harness Satin Weave Glass Fiber Reinforced
12 Composites," *Journal of Composite Materials*, 2016.
- 13 [41] M. Karkri, L. Ibos, and B. Garnier, "Comparison of experimental and simulated effective
14 thermal conductivity of polymer matrix filled with metallic spheres: Thermal contact
15 resistance and particle size effect," *J. Compos. Mater.*, vol. 49, no. 24, pp. 3017–3030,
16 2015.
- 17 [42] C. Cao, A. Yu, and Q.-H. Qin, "Evaluation of effective thermal conductivity of fiber-
18 reinforced composites," *Int. J. Archit. Eng. Constr.*, vol. 1, no. 1, pp. 14–29, 2012.
- 19 [43] M. R. Islam and A. Pramila, "Thermal Conductivity of Fiber Reinforced Composites by the
20 FEM," *J. Compos. Mater.*, vol. 33, no. 18, pp. 1699–1715, Sep. 1999.
- 21 [44] D. Kumlutaş, I. H. Tavman, and M. T. Çoban, "Thermal conductivity of particle filled
22 polyethylene composite materials," *Compos. Sci. Technol.*, vol. 63, no. 1, pp. 113–117,
23 2003.
- 24 [45] M. Jiang, I. Jasiuk, and M. Ostoja-Starzewski, "Apparent thermal conductivity of periodic
25 two-dimensional composites," *Comput. Mater. Sci.*, vol. 25, no. 3, pp. 329–338, 2002.
- 26 [46] I. Özdemir, W. a. M. Brekelmans, and M. G. D. Geers, "Computational homogenization for
27 heat conduction in heterogeneous solids," *Int. J. Numer. Methods Eng.*, vol. 73, no. 2, pp.
28 185–204, Jan. 2008.
- 29 [47] M. Jiang, K. Alzebdeh, I. Jasiuk, and M. Ostoja-Starzewski, "Scale and boundary
30 conditions effects in elastic properties of random composites," *Acta Mech.*, vol. 148, no. 1–
31 4, pp. 63–78, 2001.
- 32 [48] D. W. Abueidda, R. K. Abu Al-Rub, A. S. Dalaq, D.-W. Lee, K. A. Khan, and I. Jasiuk,
33 "Effective conductivities and elastic moduli of novel foams with triply periodic minimal
34 surfaces," *Mech. Mater.*, vol. 95, pp. 102–115, Apr. 2016.
- 35 [49] K. A. Khan and A. H. Muliana, "Fully coupled heat conduction and deformation analyses
36 of nonlinear viscoelastic composites," *Compos. Struct.*, vol. 94, no. 6, pp. 2025–2037,
37 2012.
- 38 [50] S. Torquato, *Random Heterogeneous Materials*, vol. 16. New York, NY: Springer New
39 York, 2002.
- 40 [51] K. A. Khan, S. Z. Khan, and M. A. Khan, "Effective thermal conductivity of two-phase
41 composites containing highly conductive inclusions," *J. Reinf. Plast. Compos.*, vol. 35, no.
42 21, pp. 1586–1599, Nov. 2016.
- 43 [52] S. C. Cheng and R. I. Vachon, "The prediction of the thermal conductivity of two and three
44 phase solid heterogeneous mixtures," *Int. J. Heat Mass Transf.*, vol. 12, no. 3, pp. 249–264,
45 Mar. 1969.

- 1 [53] D. J. Jeffrey, "Conduction Through a Random Suspension of Spheres," *Proc. R. Soc. Lond.*
2 *Math. Phys. Eng. Sci.*, vol. 335, no. 1602, pp. 355–367, Nov. 1973.
- 3 [54] J.-L. Auriault and H. I. Ene, "Macroscopic modelling of heat transfer in composites with
4 interfacial thermal barrier," *Int. J. Heat Mass Transf.*, vol. 37, no. 18, pp. 2885–2892, 1994.
- 5 [55] K. S. Hong, T.-K. Hong, and H.-S. Yang, "Thermal conductivity of Fe nanofluids
6 depending on the cluster size of nanoparticles," *Appl. Phys. Lett.*, vol. 88, no. 3, p. 031901,
7 Jan. 2006.
8

2019-04-10

Analytical and numerical assessment of the effect of highly conductive inclusions distribution on the thermal conductivity of particulate composites

Khan, Kamran Ahmed

SAGE

Khan K, Hajeri F, Khan M. Analytical and numerical assessment of the effect of highly conductive inclusions distribution on the thermal conductivity of particulate composites. *Journal of Composite Materials*, Volume 53, Issue 25, 2019, pp. 3499-3514

<https://doi.org/10.1177/0021998319843329>

Downloaded from Cranfield Library Services E-Repository